J Mol Model (2013) 19:1641–1650
DOI 10.1007/s00894-012-1738-z

ORIGINAL PAPER

Interactions of hydrogen molecules with complexes of lithium cation and aromatic nitrogen-containing heterocyclic anions

Yingxin Sun · Huai Sun

Received: 14 September 2012 / Accepted: 14 December 2012 / Published online: 5 January 2013

Abstract Highly stable salt functional groups consisting of lithium cation and aromatic anions ($C_nH_nN_{5-n}$–Li) are studied for hydrogen storage using ab initio calculations, force field development, and grand canonical Monte Carlo simulations. Second-order Møller–Plesset perturbation theory with the resolution of identity approximation calculations are calibrated at the CCSD(T)/complete basis set (CBS) level of theory. The calibrations on different types of binding sites are different, but can be used to correct the van der Waals interactions systematically. The anion and salt functional groups provide multiple binding sites. With increased number of nitrogen atoms in the aromatic anion, the number of binding sites increases but the average binding energy decreases. Among the functional groups considered, CHN_4-Li exhibits the largest number of binding sites (14) and a weak average binding energy of 5.7 kJ mol^{-1} with CCSD(T)/CBS correction. The calculated adsorption isotherms demonstrate that the introduction of the functional group significantly enhances hydrogen uptake despite relatively weak average binding energy. Therefore, it is concluded that searching for functional groups with the larger number of binding sites is another key factor for enhancing the hydrogen storage capacity, given that other conditions such as free volume and surface area are fixed.

Keywords Aromatic anion · Binding energy · Binding sites · Hydrogen storage · Lithium cation

Introduction

Hydrogen storage is one of the major problems in the field of hydrogen energy. Extensive efforts have been exerted on developing physical adsorption materials such as metal organic frameworks (MOFs) and covalent organic frameworks (COFs) [1–6]. Apart from being economical for manufacturing, an ideal material should have high gravimetric or volumetric uptake capacity, fast kinetics for adsorption and desorption, as well as good thermal and mechanical stability [7]. The binding energies between H_2 molecules and their framework are the widely accepted key factors that determine the adsorption capacity. Based on computer simulations, Frost et al. [8] proposed that 10–20 kJ mol^{-1} binding energy is required to meet the US DOE targets for on-board storage [9].

Lithium doping is one approach to increase binding strengths. Lithium cation (Li^+) is reportedly able to bind up to six H_2 molecules with an average binding energy (ABE) of 19.96 kJ mol^{-1} [10]. Several computational works are based on a charge-neutral model in which lithium atoms are mixed with charge-neutral materials [1–3]. Although calculations indicate that hydrogen adsorption can be enhanced significantly, this approach lacks experimental support. Early reports on hydrogen uptake enhancement by lithium doping on carbon nanotubes have revealed flaws due to impurities [4, 5]. Subsequent measurements have shown that lithium doped on pristine carbon materials such as multiwall carbon nanotubes, intercalated graphite, graphene, or graphite does not increase hydrogen uptake [5, 6]. Recent theoretical works have also raised the possibility of doping lithium on pristine carbon materials. For example, using fully correlated second-order Møller-Plesset (MP2)

Electronic supplementary material The online version of this article (doi:10.1007/s00894-012-1738-z) contains supplementary material, which is available to authorized users.

Y. Sun (✉)
School of Chemical and Environmental Engineering,
Shanghai Institute of Technology, Shanghai 200240, China
e-mail: sunyingxin0312@sit.edu.cn

H. Sun (✉)
School of Chemistry and Chemical Engineering and Key Laboratory for Thin Film and Microfabrication of Ministry of Education, Shanghai Jiao Tong University,
Shanghai 200240, China
e-mail: huaisun@sjtu.edu.cn

calculations, Ferre-Vilaplana [6] reported that the binding energy and charge transfer between lithium and graphene are so weak that the complex cannot provide a strong binding force to hydrogen.

A different approach is the chemical introduction of Li^+ to a reduction reagent. Mulfort and Hupp [11] presented a functionalized MOF with Li^+ ions. Yang et al. [12] reported that the incorporation of exposed Li^+ sites within a framework can increase the isosteric heat of H_2 adsorption. Himsl et al. [13] proposed a method to incorporate lithium alkoxide groups to organic linkers of MOFs by ion exchange. Li et al. [14] demonstrated a strategy for enhancing hydrogen storage capacity by doping conjugated microporous polymers (CMPs) with Li^+. Klopper et al. [15] reported a first-principles study on the interactions of molecular hydrogen (H_2) with lithium-substituted molecules, lithium benzide (C_6H_5Li), lithium phenoxide (C_6H_5OLi), and lithium benzoate (C_6H_5COOLi). Using the MP2/complete basis set (CBS) and CCSD(T)/CBS methods, the binding energy of H_2 with these compounds is predicted to be about 10.9 kJ mol^{-1}.

Recently, a simulation work of our group [16] introduced a new organic porous material that contains lithium tetrazolide groups. The lithium tetrazolide group is more stable and polarized than models formed by doping aromatic groups with lithium atoms. More importantly, this functional group can significantly improve the hydrogen storage capacity. The predicted hydrogen uptake reaches 5.1 wt% at 233 K and 10 MPa, exceeding the 2010 DOE target. This extraordinary performance is due not to a strong binding energy (ABE is only about 5–6 kJ mol^{-1}), but to the large number of bonding sites that the functional group provides.

In the present paper, the work of our group is extended by considering a group of aromatic, five-membered ring anions with different numbers of nitrogen atoms and Li^+, $C_nH_nN_{5-n}Li$ [n=1−5]. Different basis sets used in the MP2 perturbation theory with the resolution of identity (RI) approximation (RI-MP2) [17] calculations were examined. A suitable basis set for describing hydrogen binding energies was identified by comparing the RI-MP2 results against the ab initio limiting data obtained by the CCSD(T) method [18] and extrapolated CBS [19]. The purpose was to establish a procedure for any proposed functional group wherein similar calculations are performed to establish the baseline data for developing force field parameters. The force field is then used with grand canonical Monte Carlo (GCMC) simulations to predict hydrogen uptake.

Computational details

The structures of the aromatic anions ($C_nH_nN_{5-n}^-$) and their lithium salt molecules ($C_nH_nN_{5-n}Li$) were optimized using the density functional theory (DFT) with the B3LYP hybrid density functional [20] and 6–31+G(d,p) basis set. The optimized structures were verified by performing frequency calculations. To determine the dissociation energies of the salt molecules, single-point energies on the DFT-optimized structures were obtained using the RI-MP2/cc-pVQZ method for comparison with the DFT results. The dissociation energy of a salt molecule is the energy required to break the salt into corresponding ions at infinite separation.

The structures of the hydrogen-bonded clusters were optimized using the RI-MP2 [17] method without symmetry constraints. The self-consistent field (SCF) convergence criterion was set at 10^{-8} a.u., and the SCF density was converged to 10^{-8}. The optimizations were performed using the def2-TZVPP basis set with the corresponding auxiliary basis set for RI approximation [17]. The stationary points of the optimized structures were verified by performing numerical frequency calculations. Using the optimized structures, the binding energies between the ionic (anion or salt) group and H_2 were calculated using various basis sets, including 6–31+G(d,p), 6–311++G(2d,2p), TZVPP, QZVPP, cc-pVTZ, and cc-pVQZ. The binding energies were also calculated in two steps using the CCSD(T) correlation and CBS. First, the RI-MP2 energies based on Dunning's correlation-consistent basis sets (cc-pVTZ and cc-pVQZ) were calculated. These energies were then extrapolated to the CBS limit by applying the two-point Helgaker extrapolation scheme [19]:

$$E_{MP2}^{CBS} = \frac{E_{MP2}^{X}X^3 - E_{MP2}^{Y}Y^3}{X^3 - Y^3}, \quad (1)$$

where X=3 and Y=4 are for the cc-pVTZ and cc-pVQZ basis sets, respectively. The CCSD(T) limiting energies were then obtained using the additive scheme [15]:

$$E_{CCSD(T)}^{CBS} = E_{MP2}^{CBS} + \left(E_{CCSD(T)}^{X} - E_{MP2}^{X}\right), \quad (2)$$

where the last term is calculated with the smaller basis set (X = cc-pVQZ). The basis set superposition error (BSSE) in the calculated binding energies was corrected using the standard counterpoise correction method of Boys and Bernardi [21]. All the E_{MP2}^{X}, E_{MP2}^{Y}, and $E_{CCSD(T)}^{X}$ represent total electronic energies.

The total binding energy (TBE) and ABE per molecule were defined for analysis. The TBE for a cluster was calculated as the energy difference between the monomers (ionic species and H_2) and cluster. The ABE of a cluster was computed by dividing the TBE with the number of H_2 molecules in the cluster. The ABE could describe the average binding ability of a cluster for hydrogen molecules.

A force field representing the interactions between H_2 and the functional groups was derived based on the calibrated ab initio energy data. The rigid model was used in the force

field calculations so that the interaction energies were represented by the pairwise Coulomb and Lennard-Johns (LJ) 12–6 terms:

$$E(r_{ij}) = E_{LJ} + E_{coul} = 4\varepsilon_{ij}\left[\left(\frac{\sigma_{ij}}{r_{ij}}\right)^{12} - \left(\frac{\sigma_{ij}}{r_{ij}}\right)^{6}\right] + \frac{q_i \cdot q_j}{r_{ij}}. \quad (3)$$

The Lorentz-Berthelot combination rule was used to construct parameters for different atom pairs:

$$\varepsilon_{ij} = \sqrt{\varepsilon_i \varepsilon_j} \qquad \sigma_{ij} = \frac{\sigma_i + \sigma_j}{2}. \quad (4)$$

For H_2, the Darkrim and Levesque (DL) potential function [22] was used. In the DL model, the H-H bond length is fixed at 0.0741 nm. The LJ interaction site (σ_i=2.96 Å and ε_i=0.3051 kJ mol^{-1}) is placed at the center of the mass, and three-point charges are placed on the nucleus (q_i=0.4664) and at the center of mass (q_i=−0.9328), representing the quadruple moment of a H_2.

Using the force field, the hydrogen adsorption isotherms and isosteric heat values were calculated using GCMC simulations [23, 24]. The simulation techniques are explained in our previous study [16]. The DFT calculations were performed using the Gaussian 03 program [25]. The RI-MP2 and CCSD(T) calculations were performed using the TURBOMOLE 6.2 program [26]. The MC simulations were carried out using the Towhee 4.16.8 program [27].

Results and discussion

Interaction of Li^+ with aromatic heterocyclic anions

Figure 1 shows the B3LYP/6–31+G(d,p)-optimized structures of the salt molecules that consist of Li^+ and aromatic five-membered rings with different numbers of nitrogen atoms. Li^+ has two possible positions relative to the five-membered ring: out-of-plane and in-plane. For the out-of-plane structures, the lithium atom is above the ring but inclined to nitrogen atoms if they exist. The distances between the lithium and ring plane range from 1.754 Å to 1.850 Å. The in-plane structures are formed by the bonding between the lithium and nitrogen atoms. If nitrogen is between two carbon atoms in the five-membered ring, lithium is bonded to nitrogen and the distances vary from 1.804 Å to 1.819 Å. If two or more nitrogen atoms are adjacent, they share a lithium atom and the bond distances range from 1.829 Å to 1.874 Å.

Molecules that consist of Li^+ and aromatic anions are very stable, as evidenced by their dissociation energies

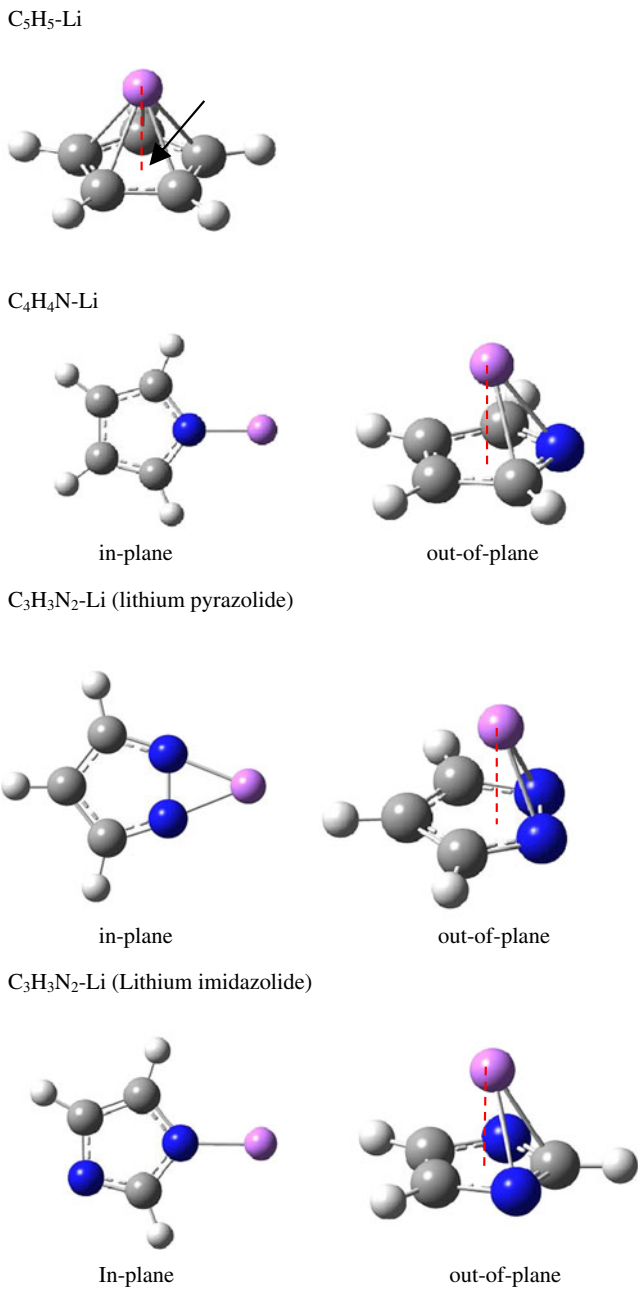

Fig. 1 B3LYP/6–31+G(d,p) optimized structures of $C_nH_nN_{5-n}$–Li isomers [n=1−5]. The lithium, nitrogen, carbon and hydrogen atoms are colored by *violet*, *blue*, *grey*, and *white*. The *dotted line* represents the vertical distance from Li atom to aromatic ring plane

(Table 1). The binding energies obtained at the B3LYP functional are similar to those obtained at the MP2 level; the order of magnitude and trend of variation of these energies are the same. The largest relative deviation of the binding energy between B3LYP and RI-MP2/vqz is less than 3 %. These results verify that the B3LYP functional is sufficient for predicting the relative strength of ionic interactions. Interestingly, the binding energies at the RI-MP2 level with RI approximation

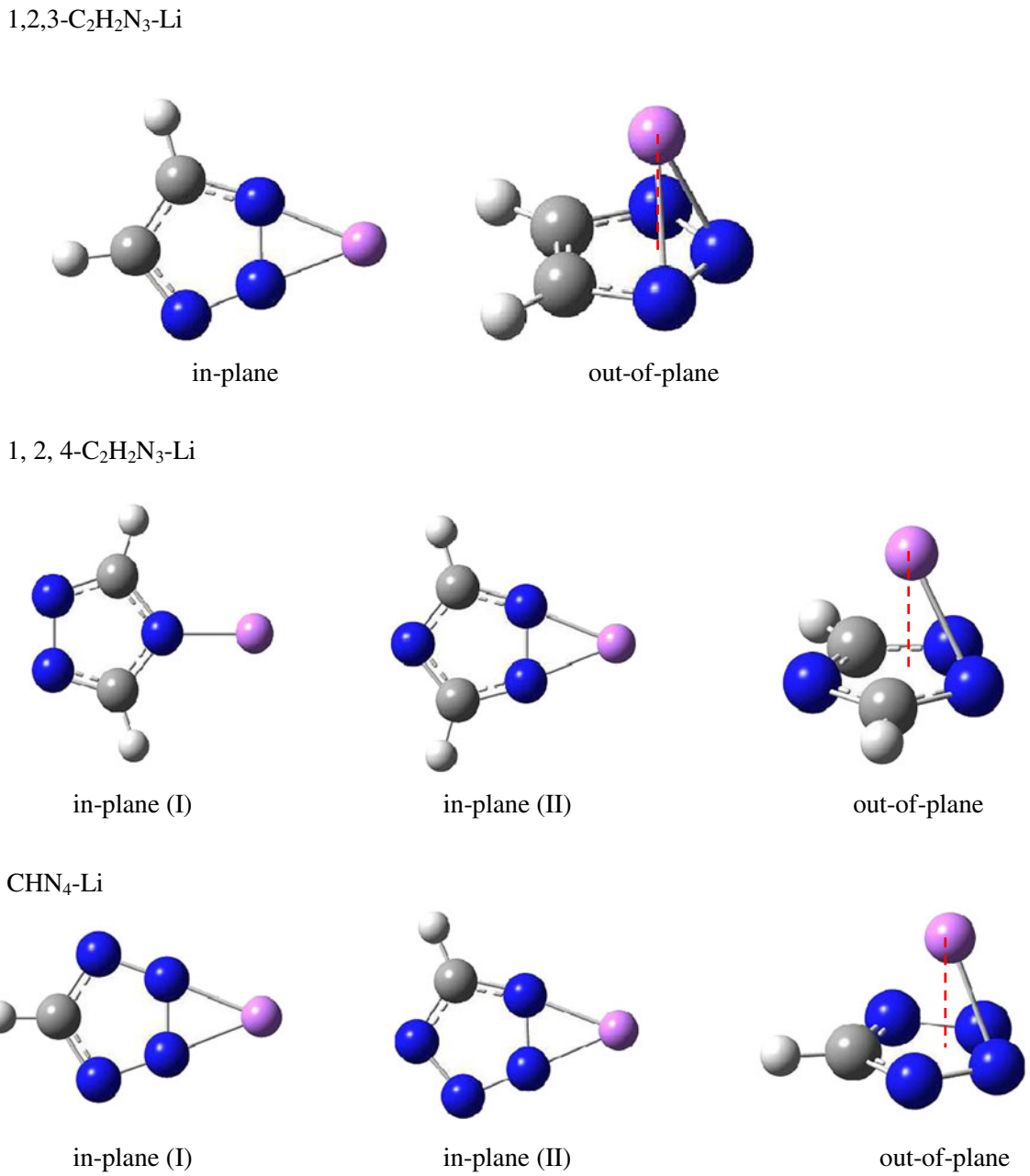

Fig. 1 (continued)

are slightly higher than those at the conventional MP2 level based on the calculation of four-center integrals. Relatively speaking, the B3LYP functional predicts higher binding energies than conventional MP2 and RI-MP2 methods.

The different predicted stabilities for different isomers of lithium complexes in Table 1 exhibit certain patterns. With increased number of nitrogen atoms in the ring, the binding energy decreases. The introduction of carbon atoms to the ring enhances the binding energy between nitrogen and lithium. The in-plane pyrazolide $C_3H_3N_2$−Li exhibits a higher binding energy than the out-of-plane isomer. The binding energy is related to the number of nitrogen atoms directly involved in the bond. The large atomic charges (more than 0.9 e) on Li indicate the ionic bonding in nature between Li^+ and the aromatic anions. For the out-of-plane lithium isomers, the NPA charge on Li increases from 0.909e to 0.934e with increased number of nitrogen atoms. For the in-plane lithium isomers, the trend is the same but the changes are smaller.

The dissociation energies and charge separations are much stronger than those obtained for the charge-neutral complex of lithium and aromatic rings [6]. To perform a direct comparison, we optimized the lithium-benzene

Table 1 Dissociation energies (in kJ mol^{-1}) of the salt molecules consisting of aromatic anion and lithium cation, calculated using B3LYP, conventional MP2, and RI-MP2 methods with cc-pVQZ basis sets and BSSE corrections on structures optimized using B3LYP/6–31+G(d,p), MP2/6–311G(2df), and RI-MP2/def2-TZVPP methods respectively. The def2-TZVPP is comparable to 6–311G(2df). The atomic charges on the Li^+ are NPA charges calculated at the B3LYP/6–31+G(d,p) level

Cluster	Isomer	DFT	MP2	RI-MP2	Q(Li^+)
C_5H_5-Li	C_5H_5-Li	719.1	702.1	711.5	0.909
C_4H_4N-Li	in-plane	643.8	627.5	631.3	0.960
	out-of-plane	688.4	671.3	680.2	0.916
$C_3H_3N_2$-Li (pyrazolide)	in-plane	710.2	689.6	695.5	0.944
	out-of-plane	662.0	645.3	653.3	0.923
$C_3H_3N_2$-Li (imidazolide)	in-plane	622.4	602.7	606.5	0.954
	out-of-plane	648.7	634.9	643.2	0.929
$C_2H_2N_3$-Li (1, 2, 3-triazolide)	in-plane	677.7	655.4	661.1	0.933
	out-of-plane	629.8	612.2	619.7	0.925
$C_2H_2N_3$-Li (1, 2, 4-triazolide)	in-plane (I)	587.1	572.6	576.2	0.958
	in-plane (II)	673.4	654.6	660.3	0.939
	out-of-plane	618.6	602.8	610.2	0.934
CHN_4-Li	in-plane (I)	632.2	617.8	623.1	0.934
	in-plane (II)	632.1	612.6	618.0	0.941
	out-of-plane	586.6	572.0	578.8	0.934

complex using the RI-MP2/cc-pVQZ method. The binding energy is only 15 kJ mol^{-1} and the NPA charge is 0.012e on lithium. This finding is consistent with that reported through fully correlated MP2 calculations performed on Li for a Li/graphene model compound with a binding energy of 12.5 kJ mol^{-1} and a charge transfer of −0.06e [6].

Selection of basis set for weak binding energy predictions

To describe weak interactions with H_2, a number of computational methods are compared with the CCSD(T)/CBS results. The ABE values calculated using different methods and basis sets are summarized in Table 2. This study was conducted using tetrazolide anion (CHN_4^-) and the in-plane lithium complex (CHN_4Li) as a model compound representing two typical binding sites, i.e., aromatic nitrogen and Li^+, respectively. For nitrogen, the ABE was calculated using two bound H_2. For Li^+, the ABE was calculated with four bound H_2. The B3LYP/6–31+G(d,p) method underestimated the ABE by more than 2 kJ mol^{-1}. In the RI-MP2 calculations, the calculated ABE values increased with increased size of the basis set. The effect of the high-level electron correlation (from MP2 to CCSD(T)) is slightly more complicated. With a small basis set (TZVPP), the effect of the high-level correlation is not very clear; however, with a large basis set, the high-level correlation makes the ABE slightly weaker for the anion but stronger for the salt. Using CCSD(T)/CBS as the benchmark, one of the RI-MP2 methods can be used with known systematic errors. In our previous work, RI-MP2/TZVPP data were selected for developing force field parameters. Table 2 shows that the ABE values are −0.6 and −1.4 kJ mol^{-1} weaker than the CCSD(T)/CBS results for the aromatic nitrogen and Li^+ sites, respectively. If the RI-MP2/cc-pVQZ method is used, the ABE errors are about 0.1 kJ mol^{-1} for the nitrogen site and −0.4 kJ mol^{-1} for the Li^+ site and the method is used for all calculations in this paper. The introduction of diffusion function for Li^+ does not improve the accuracy of binding energies (See Table S8 in the Supporting information, SI).

Table 2 Comparison of ABE (in kJ mol^{-1}) calculated using different ab initio methods. Two models, tetrazolide anion (CHN_4^-) and lithium tetrazolide (CHN_4−Li) are used for representing two typical binding sites. All data include the BSSE corrections

Methods	CHN_4^-	CHN_4−Li
B3LYP/6–31+G(d,p)	6.2	5.6
MP2/6–311++G(2d,2p)	7.2	8.1
RI-MP2/TZVPP	**7.5**	**9.0**
RI-MP2/QZVPP	8.0	9.9
RI-MP2/cc-pVTZ	8.0	9.5
RI-MP2/cc-pVQZ	**8.2**	**10.0**
RI-MP2/CBS	8.3	10.5
CCSD(T)/TZVPP	7.6	8.9
CCSD(T)/cc-pVQZ	8.0	10.0
CCSD(T)/CBS	**8.1**	**10.4**

The best MP2 method obviously depends on the interaction sites to be calculated. Hüber et al. [28] reported that for H_2 with substituted benzene C_6H_5X (X = H, F, OH, etc.), the energy data obtained using the RI-MP2/TZVPP method are close to those obtained using CCSD(T)/TZVPP and BSSE corrections. Klopper et al. [15] reported that for lithium containing benzene molecules (C_6H_5Li, C_6H_5OLi, and C_6H_5COOLi), the MP2 method with a complete basis set

(MP2/CBS) is adequate and the CCSD(T) method does not significantly change the binding energy.

Interactions of hydrogen with the anions

The aromatic anions provide multiple binding sites for H_2. Figure S1 shows the optimized structures of the complexes of H_2 and $C_nH_nN_{5-n}^-$ [n=1−5] anions. The structures represent possible configurations with the maximum number of H_2 molecules in direct contact with the anions. These structures were obtained by adding H_2 molecules one-by-one to minimize the possibility of reduction to the local minimum. The structures show that each nitrogen atom binds to two H_2 molecules, and each side of the aromatic ring binds one. The distances denoted are those between the hydrogen atoms and the nearest nitrogen or ring plane. The H_2 molecules are oriented in a "head-on" fashion toward the interaction site, and the distances generally range within 2.3–2.6 Å.

The binding energies are fairly strong between aromatic anions and H_2. Figure 2 summarizes the TBE as a function of the number of H_2 molecules (more specific data are given in the SI). For each anion, the TBE scales up linearly at roughly constant increments. Therefore, the binding sites are more or less equivalent, there is no clear order in which the binding sites are occupied. The slopes (corresponding to ABE values) of the curves vary for different species.

The ABE values are tabulated in Table 3. Although the maximum number of adsorbed H_2 molecules increases with the number of nitrogen atoms, the ABE decreases. The anion with the greatest number of binding sites, CHN_4^-, exhibits the lowest ABE of 7.0 kJ mol^{-1}. The anion that provides the fewest binding sites, $C_5H_5^-$, has the highest binding energy of 14.1 kJ mol^{-1}.

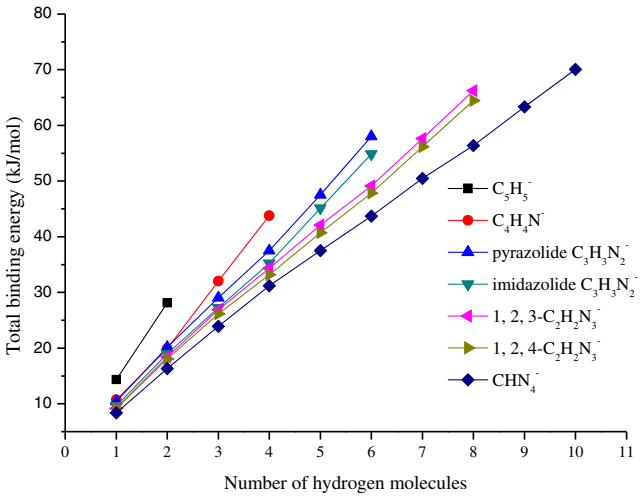

Fig. 2 TBE of H_2 molecules with $C_nH_nN_{5-n}^-$ anions as the number of H_2 molecules, calculated at the level of RI-MP2/cc-pVQZ

Table 3 The ABE (in kJ mol^{-1}) calculated for hydrogen molecules bound to aromatic anions calculated at the RI-MP2/cc-pVQZ level of theory. The average dipole moments (Debye) and bond lengths (Å) of the hydrogen molecules are listed for comparison

Models	ABE	$\overline{\mu}$	$\overline{R}$
$C_5H_5^-$	14.1	0.248	0.748
$C_4H_4N^-$	11.0	0.245	0.750
pyrazolide $C_3H_3N_2^-$	9.7	0.233	0.749
imidazolide $C_3H_3N_2^-$	9.2	0.228	0.749
1, 2, 3-$C_2H_2N_3^-$	8.3	0.212	0.748
1, 2, 4-$C_2H_2N_3^-$	8.1	0.213	0.748
tetrazolide CHN_4^-	7.0	0.193	0.747

H_2 molecules are lined up toward the binding sites (Fig. S1); thus, the induced dipoles of hydrogen can be calculated using atomic charges and bond lengths:

$$\overline{\mu} = \frac{1}{n}\sum_{i=1}^{n} r_i \times \left|\overline{Q}_H^i\right|,$$

where n is the total number of adsorbed H_2 molecules on each specie, r_i is the bond length of the ith H_2 molecule, and $\left|\overline{Q}_H^i\right|$ is the average absolute charge of two hydrogen atoms for the ith H_2 molecule. The results listed in Table 3 indicate that the H-H bond lengths are very similar. However, the induced dipole moments of the adsorbed H_2 molecule decrease with increased number of nitrogen atoms in the aromatic ring from $C_5H_5^-$ to CHN_4^- anions, indicating the decreased polarization ability of $C_nH_nN_{5-n}^-$ anions. This trend is consistent with the binding energies.

Interaction of hydrogen and lithium salt complexes $C_nH_nN_{5-n}$–Li [n=1−5]

Salt molecules bind more H_2 molecules than their corresponding anion species because both anions and cations provide binding sites. Figure S2 shows the optimized structures of the salts in direct contact with the maximum number of H_2 molecules. The pattern of the maximum number of H_2 molecules can be described as follows. Five H_2 molecules interact with Li^+ connected with one nitrogen atom. Four H_2 molecules interact with Li^+ bound to two nitrogen atoms. Three H_2 molecules interact directly with out-of-plane Li^+. Each exposed nitrogen atom (no directly bound Li^+) binds two H_2 molecules. Each side of the ring binds one H_2 molecule. Up to 14 sites exist for in-plane CHN_4–Li.

The binding sites are no longer equivalent based on the changes in the slopes of the TBE curves in Fig. 3. The TBE values shown are for 3a) out-of-plane, 3b) in-plane with the Li cation bonded to one nitrogen, and 3c) in-plane with the Li cation bonded to two nitrogen atoms. There are slope transitions in most of the curves, indicating the changes in ABE. For all complexes, the initial binding sites that are also the strongest binding sites are the Li^+ sites. Other binding sites are populated only after the Li^+ sites are saturated.

The ABE values are classified as Li^+ sites, anion sites, overall average, and overall average with CCSD(T)/CBS corrections in Table 4. The data are grouped in the same way as those in Fig. 3. For the out-of-plane lithium complexes (corresponding to Fig. 3a), the ABE for Li depends on the number of nitrogen atoms in the complexes, ranging from 7.1 to 12.6 kJ mol^{-1}. More nitrogen atoms in the complexes result in higher ABE values. For in-plane Li^+ with one nitrogen atom directly bonded (corresponding to Fig. 3b), the ABE values are similar and quite strong at 11.2–11.3 kJ mol^{-1}. For in-plane Li^+ with two nitrogen atoms directly bound (corresponding to Fig. 3c), the ABE values range within 8.8–10.0 kJ mol^{-1}. "A^-" refers to binding sites on the anion, where the ABE values broadly range within 3.4–8.7 kJ mol^{-1}. The "overall" ABE values calculated using the arithmetic average range within 5.7–10.6 kJ mol^{-1}. The CCSD(T)/CBS values corrected using the calibration data (see Table 2) are listed in the last column. Given the opposite corrections for the anion (+0.1 kJ mol^{-1}) and cation (−0.4 kJ mol^{-1}), the overall corrections are minimal.

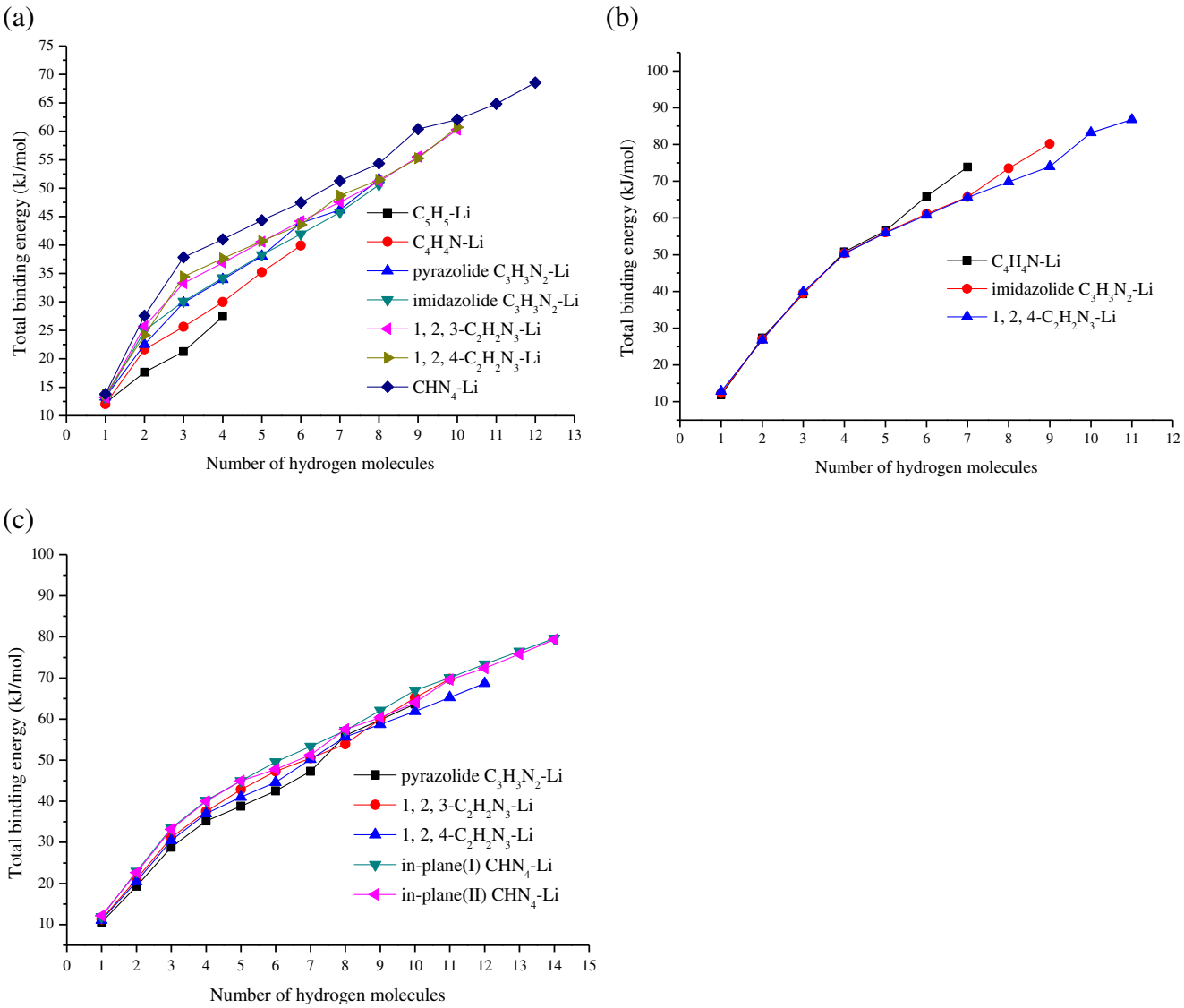

Fig. 3 TBE of H_2 with different lithium salts calculated at the level of RI-MP2/cc-pVQZ. (**a**) out-of-plane (**b**) in-plane with the Li cation bonded to one nitrogen atom and (**c**) in-plane with the Li cation bonded to two nitrogen atoms

Table 4 The ABE (in kJ mol^{-1}) and number of binding sites on: Li^+ and anion (A^-), and overall, calculated at the RI-MP2/cc-pVQZ level of theory with BSSE correction. The overall ABE are calculated by arithmetic averaging. The last column (overall*) is estimated by adding the CCSD(T)/CBS corrections

Models	Li^+	N(Li)	A^-	N(A)	Overall	Overall*
C_5H_5-Li	7.1	3	6.2	1	6.9	7.2
out-of-plane C_4H_4N-Li	8.5	3	4.8	3	6.7	6.8
out-of-plane pyrazolide $C_3H_3N_2$-Li	10.0	3	4.3	5	6.4	6.5
out-of-plane imidazolide $C_3H_3N_2$-Li	10.0	3	4.1	5	6.3	6.4
out-of-plane 1, 2, 3-$C_2H_2N_3$-Li	11.1	3	3.9	7	6.0	6.1
out-of-plane 1, 2, 4-$C_2H_2N_3$-Li	11.5	3	3.8	7	6.1	6.2
out-of-plane CHN_4-Li	12.6	3	3.4	9	5.7	5.7
in-plane C_4H_4N-Li	11.3	5	8.7	2	10.6	10.8
in-plane imidazolide $C_3H_3N_2$-Li	11.2	5	6.0	4	8.9	9.1
in-plane (I) 1, 2, 4-$C_2H_2N_3$-Li	11.2	5	5.1	6	7.9	8.0
in-plane pyrazolide $C_3H_3N_2$-Li	8.8	4	4.7	6	6.4	6.4
in-plane 1, 2, 3-$C_2H_2N_3$-Li	9.4	4	4.6	7	6.3	6.4
in-plane (II) 1, 2, 4-$C_2H_2N_3$-Li	9.3	4	4.0	8	5.7	5.8
in-plane (I) CHN_4-Li	**10.0**	**4**	**3.9**	**10**	**5.7**	**5.7**
in-plane (II) CHN_4-Li	**10.0**	**4**	**3.9**	**10**	**5.7**	**5.7**

The H_2 molecules near Li^+ are orientated in a way that they can interact with Li^+ on the side of the molecular axis (Fig. S2). Obviously, this configuration maximizes the interactions between the electron density of H_2 and the positively charged Li^+. Therefore, the interaction between H_2 and Li^+ must be charge-quadrupole dominated [15, 29–31].

Adsorption on a model material containing CHN_4Li

In our earlier work [16], the hydrogen storage capacity for the porous aromatic framework (PAF-4) with lithium tetrazolide (in-plane CHN_4Li) moieties is predicted using GCMC simulations based on a force field derived from the RI-MP2/def2-TZVPP level of theory. The data in Table 2 indicate that the ABE values obtained at this level for two typical binding sites (negatively charged aromatic nitrogen and positively charged Li^+) are about 7 % and 13 % weaker than the ab initio limiting (CCSD(T)/CBS) values. The overall underestimate is about 9 %.

Using the revised ab initio data, the force field parameters were adjusted (See Table S9 in the SI) to represent the ab initio limiting ABE, and GCMC simulations were carried out to predict the adsorption isotherms and isosteric heat of adsorption (IHA) of H_2. Despite the force field variations, the changes in the calculated isotherms and IHA values are not significant. As shown in Fig. 4, the adsorption isotherms of the two predictions using different force fields are very similar at all three temperatures (77, 233, and 298 K). The changes in the calculated IHA curves, with fluctuations, are almost the same at 77 K but slightly higher at 233 and 298 K. The increments of IHA at 233 and 298 K are about 5 % higher than the previous results, which is reasonable compared with the estimated 9 % increase in the ABE values.

The calculated isotherms are insensitive to the ABE because of complicated temperature effects. Generally, with increased temperature, the thermal motion weakens the framework-hydrogen interactions. This phenomenon is supported by the initial (very low load of hydrogen) IHA values. At 77 K, the values are close to the ABE, 10.4 kJ mol^{-1}. At 233 and 298 K, the initial IHA values are a fraction of the ABE values. On the other hand, temperature plays an opposite role associated with the amount of hydrogen loaded. At low temperatures and high pressures, the load is high (five times more at 77 K than at 233 K). The major contribution to the adsorption energy is not from the framework-hydrogen interaction but from the hydrogen-hydrogen interactions. At high temperatures, the load is low and then the framework-hydrogen interactions become more important. This finding can be verified by the calculated IHA with loaded hydrogen. At 77 K, the average IHA is slightly higher than 3 kJ mol^{-1}, which is close to the cohesive energy of hydrogen in bulk. At 233 and 298 K, the IHA values are higher, averaging between 4.5 and 4.7 kJ mol^{-1}. Given that the framework-hydrogen potential energy is undermined by the temperature effect, the predicted adsorption curves are insensitive to the changes in ABE. This result also explains why a crude potential (e.g., UFF) can be used to predict adsorption curves reasonably well, especially at high loads where the ABE is insensitive [32].

Fig. 4 Comparison of calculated gravimetric and volumetric adsorption isotherms (*left*) and isosteric heats of adsorption (*right*) for H_2 on model porous material (PAF-4) with the lithium tetrazolide moieties at (**a**) 77 K, (**b**) 233 K and (**c**) 298 K. The previous work [16] was based on a force field derived based RI-MP2/TZVPP calculations ▶

(a)

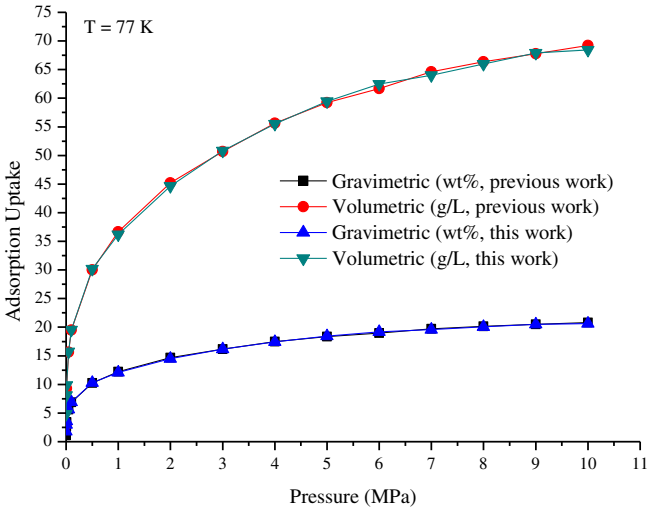
T = 77 K
Adsorption Uptake
Pressure (MPa)
Gravimetric (wt%, previous work)
Volumetric (g/L, previous work)
Gravimetric (wt%, this work)
Volumetric (g/L, this work)

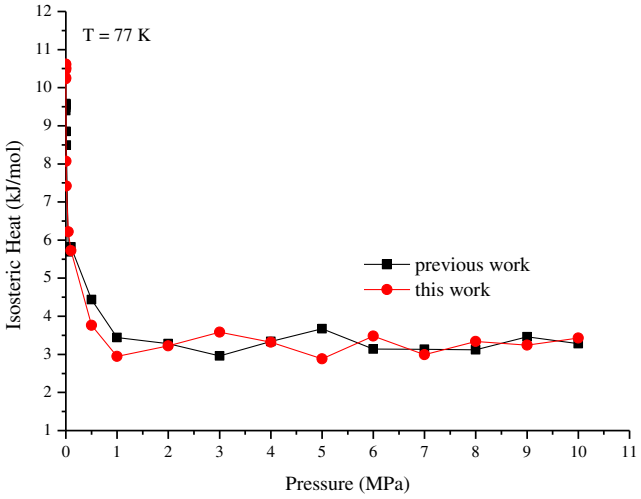
T = 77 K
Isosteric Heat (kJ/mol)
Pressure (MPa)
previous work
this work

(b)

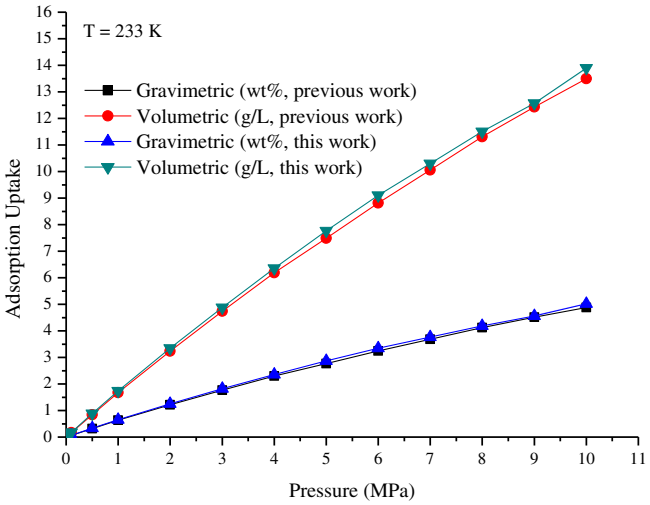
T = 233 K
Adsorption Uptake
Pressure (MPa)
Gravimetric (wt%, previous work)
Volumetric (g/L, previous work)
Gravimetric (wt%, this work)
Volumetric (g/L, this work)

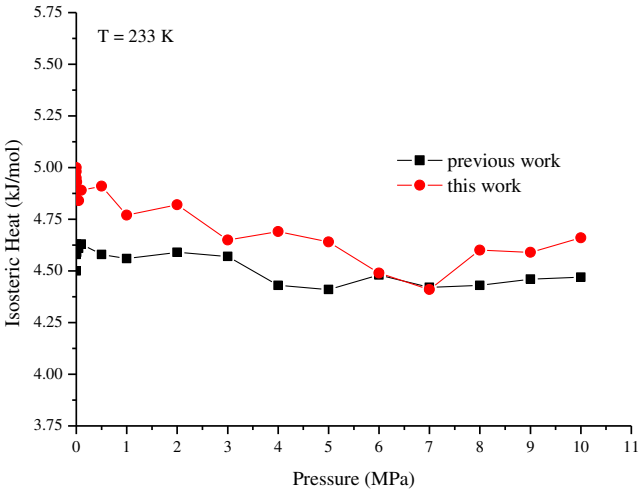
T = 233 K
Isosteric Heat (kJ/mol)
Pressure (MPa)
previous work
this work

(c)

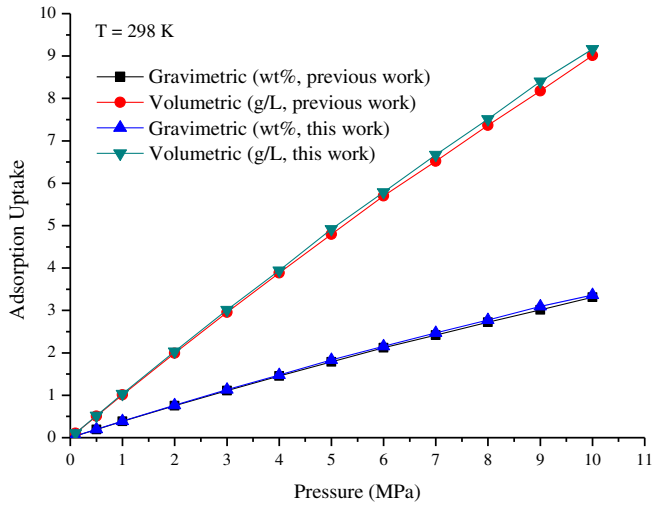
T = 298 K
Adsorption Uptake
Pressure (MPa)
Gravimetric (wt%, previous work)
Volumetric (g/L, previous work)
Gravimetric (wt%, this work)
Volumetric (g/L, this work)

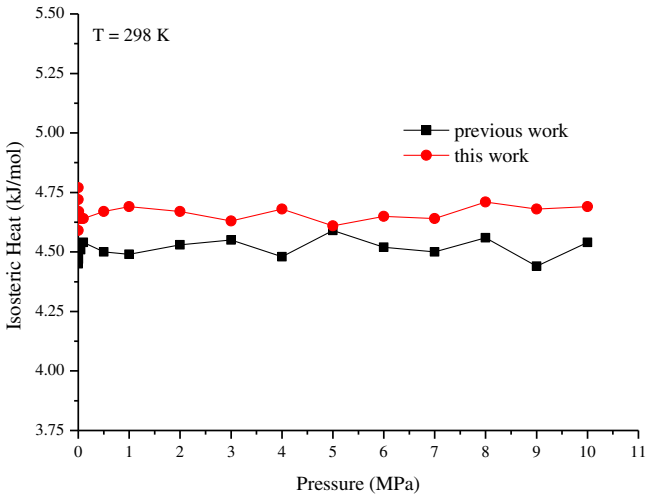
T = 298 K
Isosteric Heat (kJ/mol)
Pressure (MPa)
previous work
this work

Conclusions

The salt molecules $C_nH_nN_{5-n}$–Li that consist of lithium cation and aromatic five-membered ring anions with different numbers of nitrogen atoms are highly stable. The corresponding ionic bonds in the salt molecules can be attributed to the significant charge separation between Li cations and anions.

Using CCSD(T)/CBS calculations as benchmark, the RI-MP2 method with a reasonably large basis set can be used to characterize ABE between the functional groups and H_2 molecules with known systematic errors. In this work, the RI-MP2/cc-pVQZ method with BSSE correction was used to calculate the ABE. The systematic errors are 0.1 kJ mol^{-1} for the site of the negatively charged aromatic ring and −0.4 kJ mol^{-1} for the Li^+ site. Using these as corrections, the CCSD(T)/CBS-corrected potential surface energy can be obtained to develop force field parameters.

Both $C_nH_nN_{5-n}^-$ anion and $C_nH_nN_{5-n}$–Li salt bind H_2 with multiple sites but with weak binding energies. For $C_mH_mN_n^-$ anions, each nitrogen atom binds two H_2 molecules and each side of the aromatic ring binds one. For the $C_nH_nN_{5-n}$–Li complex, in addition to the binding sites provided by nitrogen and the ring, Li^+ provides four to five additional binding sites for H_2. The CHN_4–Li functional group provides the greatest number of binding sites (14), and the CCSD(T)/CBS-corrected ABE is 5.7 kJ mol^{-1}. Simulations performed on PAF-4 material [16] with the functional group incorporated demonstrate that the uptake at room temperature meets the requirement of the US DOE target for on-board storage, despite relatively weak ABE. Therefore, it is concluded that searching for functional groups with the larger number of binding sites is another key factor for enhancing the hydrogen storage capacity, given that other conditions such as free volume and surface area are fixed.

The factors that determine the overall uptake are complicated. The binding energy is not the only factor that needs to be considered. Our simulations indicate that a 9 % deviation in ABE does not produce significant differences in the predicted isotherm curves and IHA values because the framework-hydrogen interactions (can be described by ABE) are undermined by the temperature effects.

Acknowledgments This work was funded by the National Science Foundation of China (nos. 21203118, 21073119 and 21173146), the Scientific Research Foundation of Shanghai Institute of Technology (grant YJ2012-11), and by the National Basic Research Program of China (no. 2007CB209701).

References

1. Deng WQ, Xu X, Goddard WA (2004) Phys Rev Lett 92:166103
2. Han SS, Goddard WA (2007) J Am Chem Soc 129:8422–8423
3. Cao DP, Lan JH, Wang WC, Smit B (2009) Angew Chem Int Ed 48:4730–4733
4. Chen P, Wu X, Lin J, Tan KL (1999) Science 285:91–93
5. Pinkerton FE, Wicke BG, Olk CH, Tibbetts GG, Meisner GP, Meyer MS, Herbst JF (2000) J Phys Chem B 104:9460–9467
6. Ferre-Vilaplana A (2008) J Phys Chem C 112:3998–4004
7. Schlapbach L, Züttel A (2001) Nature 414:353–358
8. Frost H, Snurr RQ (2007) J Phys Chem C 111:18794–18803
9. U.S. Department of Energy. Energy Efficiency and Renewable Energy. http://www1.eere.energy.gov/hydrogenandfuelcells/storage/pdfs/targets_onboard_hydro_storage.pdf
10. Barbatti M, Jalbert G, Nascimento MAC (2001) J Chem Phys 114:2213–2218
11. Mulfort KL, Hupp JT (2007) J Am Chem Soc 129:9604–9605
12. Yang SH, Lin X, Blake AJ, Walker GS, Hubberstey P, Champness NR, Schröder M (2009) Nat Chem 1:487–493
13. Himsl D, Wallacher D, Hartmann M (2009) Angew Chem Int Ed 48:4639–4642
14. Li A, Lu RF, Wang Y, Wang X, Han KL, Deng WQ (2010) Angew Chem Int Ed 49:3330–3333
15. Mavrandonakis A, Klopper W (2008) J Phys Chem C 112:11580–11585
16. Sun YX, Ben T, Wang L, Qiu SL, Sun H (2010) J Phys Chem Lett 1:2753–2756
17. Weigend F, Häser M (1997) Theor Chem Acc 97:331–340
18. Raghavachari K, Trucks GW, Pople JA, Head-Gordon M (1989) Chem Phys Lett 157:479–483
19. Halkier A, Helgaker T, Jørgensen P, Klopper W, Koch H, Olsen J, Wilson AK (1998) Chem Phys Lett 286:243–252
20. Becke AD (1993) J Chem Phys 98:5648–5652
21. Boys SF, Bernardi F (1970) Mol Phys 19:553–566
22. Darkrim F, Aoufi A, Malbrunot P, Levesque D (2000) J Chem Phys 112:5991
23. Landau D, Binder K (2000) A guide to Monte Carlo simulations in statistical physics. Cambridge University Press, Cambridge, UK
24. Allen MP, Tildesley DJ (1987) Computer simulation of liquids. Oxford University Press, New York
25. Frisch MJ, Trucks GW, Schlegel HB, Scuseria GE, Robb MA, Cheeseman JR Jr, Montgomery JA, Vreven T, Kudin KN, Burant JC, Millam JM, Iyengar SS, Tomasi J, Barone V, Mennucci B, Cossi M, Scalmani G, Rega N, Petersson GA, Nakatsuji H, Hada M, Ehara M, Toyota K, Fukuda R, Hasegawa J, Ishida M, Nakajima T, Honda Y, Kitao O, Nakai H, Klene M, Li X, Knox JE, Hratchian HP, Cross JB, Bakken V, Adamo C, Jaramillo J, Gomperts R, Stratmann RE, Yazyev O, Austin AJ, Cammi R, Pomelli C, Ochterski JW, Ayala PY, Morokuma K, Voth GA, Salvador P, Dannenberg JJ, Zakrzewski VG, Dapprich S, Daniels AD, Strain MC, Farkas O, Malick DK, Rabuck AD, Raghavachari K, Foresman JB, Ortiz JV, Cui Q, Baboul AG, Clifford S, Cioslowski J, Stefanov BB, Liu G, Liashenko A, Piskorz P, Komaromi I, Martin RL, Fox DJ, Keith T, Al-Laham MA, Peng CY, Nanayakkara A, Challacombe M, Gill PMW, Johnson B, Chen W, Wong MW, Gonzalez C, Pople JA (2004) Gaussian 03. Gaussian Inc, Wallingford
26. Ahlrichs R, Bär M, Häser M, Horn H, Kölmel C (1989) Chem Phys Lett 162:165–169
27. Martin MG (2006) MCCCS Towhee, http://towhee.sourceforge.net/
28. Hübner O, Glöss A, Fichtner M, Klopper W (2004) J Phys Chem A 108:3019–3023
29. Chandrakumar KRS, Ghosh SK (2007) Chem Phys Lett 447:208–214
30. Vitillo JG, Damin A, Zecchina A, Ricchiardi G (2005) J Chem Phys 122:114311
31. Vitillo JG, Damin A, Zecchina A, Ricchiardi G (2006) J Chem Phys 124:224308
32. Garberoglio G, Skoulidas AI, Johnson JK (2005) J Phys Chem B 109:13094–13103